Z. Phys. B - Condenset Matter 62, 413-421 (1986)

Condensed Matter
Zeitschrift für Physik B

Neutron Scattering from a Substitutional Mass Defect

R.D. Williams and S.W. Lovesey
Rutherford Appleton Laboratory, Oxfordshire, United Kingdon

Received June 13, 1985

The dynamic structure factor is calculated for a low concentration of light mass scatterers substituted in a cubic crystal matrix. A new numerical method for the exact calculation is demonstrated. We derive a local density of states for the low momentum transfer limit, and derive the shifts and widths of the oscillator peaks in the high momentum transfer limit. We discuss the limitations of an approximation which decouples the defect from the lattice.

1. Introduction

The motion of single particles in non-degenerate condensed matter can be observed in inelastic neutron scattering experiments. The technique is most useful for particles with a large incoherent nuclear cross-section. A particularly important example is that of the proton, whose function is vital in many macromolecular and solid state systems. Fortunately, the proton incoherent cross-section is exceptionally large.

Theoretical models based on harmonic particle motion are often a good first approximation to particle motion in molecules and solids. The single particle motion in some harmonic models can be calculated without further approximation [1–3]. A full appreciation of the features of such models is an essential prelude to a complete interpretation of neutron scattering measurements.

Here we present a comprehensive study of the response that would be observed in scattering from a particle embedded in a harmonic matrix. The response function is obtained in closed form and a complete study demands recourse to numerical analysis, but two physically significant limits can be studied analytically. If the neutron scattering vector is very large the response is approximately a Gaussian function of the energy transfer, which is then similar to the response of a free particle. In the opposite limiting case of small scattering vectors a mode expansion is appropriate, and the response can be attributed to an elastic contribution, and contributions from the fundamental and higher-order modes. For intermediate scattering vectors, the response contains a wealth of structure that partly reflects prominent features in the vibrational density of states of the host matrix that arise from the Van Hove singularities. We compare results for a Debye density of states with a realistic density of states to illustrate the shortcomings of the Debye model. Effects of temperature and scattering vector are reported in detail.

2. Response Function

Let us denote the change in wave vector and frequency of the neutrons by $\mathbf{Q}$ and ω, respectively. If the position vector of the a'th particle is $\mathbf{R}_a$, the response observed in incoherent scattering from particle a is the time Fourier transform of [2]

$$F_a(\mathbf{Q}, t) = \langle \exp(-i\mathbf{Q}\cdot\mathbf{R}_a) \exp(i\mathbf{Q}\cdot\mathbf{R}_a(t)) \rangle. \tag{2.1}$$

Here, $\mathbf{R}_a(t)$ is the Heisenberg operator at time t, and $\mathbf{R}_a(0) \equiv \mathbf{R}_a$. Note that the position operators do not commute at different times.

Several properties of $F_a(\mathbf{Q}, t)$ merit discussion at this point. First, $F_a(\mathbf{Q}, t) = F_a(-\mathbf{Q}, t)$ which follows from time reversal. Since the position operators in (2.1)

commute for $t=0$ it follows that,

$$F_a(\mathbf{Q},0)=1. \tag{2.2}$$

Finally, the so-called f-sum rule follows from the result,

$$\begin{aligned}&i\hbar\partial_t F_a(\mathbf{Q},t)|_{t=0}\\&=\tfrac{1}{2}\langle[\exp(-i\mathbf{Q}\cdot\mathbf{R}_a),[\exp(i\mathbf{Q}\cdot\mathbf{R}_a),H]]\rangle,\end{aligned} \tag{2.3}$$

where H is the total Hamiltonian that describes the system of particles. The proof of (2.3) utilizes the invariance of $F_a(\mathbf{Q},t)$ under $\mathbf{Q}\to-\mathbf{Q}$. If the particles interact through a potential that depends on particle positions and not their velocities, the commutator on the right-hand side of (2.3) involves only the kinetic energy operator. We find the usual f-sum rule,

$$i\partial_t F_a(\mathbf{Q},t)|_{t=0}=-\hbar Q^2/2M_a. \tag{2.4}$$

The observed response is proportional to

$$S_a(\mathbf{Q},\omega)=\frac{1}{2\pi\hbar}\int_{-\infty}^{\infty}dt\,F_a(\mathbf{Q},t)e^{-i\omega t} \tag{2.5}$$

and from (2.2) and (2.4) we deduce the frequency sum rules

$$\hbar\int_{-\infty}^{\infty}d\omega\,S_a(\mathbf{Q},\omega)=1 \tag{2.6}$$

and

$$\int_{-\infty}^{\infty}d\omega\,\omega S_a(\mathbf{Q},\omega)=Q^2/2M_a. \tag{2.7}$$

The harmonic approximation to particle motion is useful for small displacements $\mathbf{u}$ about equilibrium positions. In this instance,

$$F_a(\mathbf{Q},t)=\exp\{\langle\mathbf{Q}\cdot\mathbf{u}_a\mathbf{Q}\cdot\mathbf{u}_a(t)-(\mathbf{Q}\cdot\mathbf{u}_a)^2\rangle\}. \tag{2.8}$$

The reduction of (2.1) to (2.8) is exact for harmonic displacements; a proof is given in [2], for example. The condition (2.2) is evidently satisfied by (2.8), and (2.4) is equivalent to the condition

$$\langle\mathbf{Q}\cdot\mathbf{u}_a\mathbf{Q}\cdot\mathbf{p}_a\rangle=i\hbar Q^2/2 \tag{2.9}$$

where $\mathbf{p}_a$ is the momentum operator conjugate to the displacement $\mathbf{u}_a$. If the a'th particle inhabits a centro-symmetric environment (2.9) reduces to

$$\langle\mathbf{u}_a\cdot\mathbf{p}_a\rangle=3i\hbar/2. \tag{2.10}$$

which is a statement that the isotropic harmonic oscillator has minimum uncertainty.

3. Lattice Green Function

Most discussions of the properties of mixed crystals are couched in terms of Green functions [3–5]. In view of this, we express the correlation function in (2.8) in terms of a displacement Green function even though the problem of a single mass defect, treated here, hardly warrants use of the Green function formalism [1].

The displacement Green function is

$$G_{\alpha\beta}(l,l';\omega)=-i\int_0^{\infty}dt\langle[u_l^{\alpha}(t),u_{l'}^{\beta}(0)]\rangle e^{i\omega t} \tag{3.1}$$

where $\mathbf{u}_l(t)$ is the displacement relative to the site labelled by l; α, β denote Cartesian coordinates, and $[\ ,\ ]$ is a commutator. The displacement correlation function is obtained from the imaginary part of the Green function evaluated in the limit $\omega\to\omega+i0^+$. The relation appropriate for our calculation is derived from the fluctuation-dissipation theorem, and we find

$$\begin{aligned}&F_a(\mathbf{Q},t)\\&=\exp\left\{-\frac{1}{\pi}\int_0^{\infty}d\omega J(\omega,t)\sum_{\alpha\beta}Q_\alpha Q_\beta\,\mathrm{Im}\,G_{\alpha\beta}(a,a;\omega)\right\}\end{aligned} \tag{3.2}$$

where $\beta=1/k_BT$, and $\hbar=1$, and

$$J(\omega,t)=[\cosh\omega(it+\beta/2)-\cosh\omega\beta/2]/\sinh\omega\beta/2. \tag{3.3}$$

In deriving (3.2) we have exploited the fact that the imaginary part of the Green function is an odd function of frequency [2].

Mass and spring constant defects in various crystal structures are discussed in detail in reference [3]. Expression (3.2) provides the link between the displacement Green function derived for these problems and the correlation function in the response function observed in incoherent neutron scattering. We will consider the problem of a single mass defect in a cubic host. This simple problem illustrates a wealth of features that will be present to some extent in more complicated problems.

We now write the Green function for crystal-with-defect, G, in terms of the unperturbed Green function $P_{\alpha\beta}(l,l';\omega)$. There are two natural basis sets, one labelled by a site l and axis α, the other by wave vector $\mathbf{q}$ and phonon branch j. Since each unit cell of the crystal is assumed to have one atom of mass M, j runs from 1 to 3. The unperturbed Green function is diagonal in this latter basis, and is

$$P_{\alpha\beta}(l,l';\omega)=\frac{1}{NM}\sum_{j\mathbf{q}}\sigma_\alpha^j(\mathbf{q})\sigma_\beta^j(\mathbf{q})\frac{\exp(i\mathbf{q}\cdot(l-l'))}{\omega^2-\omega_j^2(\mathbf{q})} \tag{3.4}$$

where $\sigma^j(\mathbf{q})$ and $\omega_j(\mathbf{q})$ are the eigen vector (polarisation) and eigen value (dispersion relation) for the normal coordinate labelled by $j, \mathbf{q}$.
For cubic crystals, to which we restrict our attention, the unperturbed Green function is independent of the Cartesian labels [3]. Since

$$\sum_j \sigma_\alpha^j(\mathbf{q})\sigma_\beta^j(\mathbf{q}) = \delta_{\alpha\beta} \tag{3.5}$$

we must have $|\sigma_\alpha^j|^2 = 1/3$ for all α. It is convenient to introduce the function

$$P(\omega) \equiv M P_{\alpha\alpha}(l, l; \omega) = \frac{1}{3N} \sum_{j\mathbf{q}} (\omega^2 - \omega_j^2(\mathbf{q}))^{-1} \tag{3.6}$$

which can be expressed in terms of the normalised density of states $Z(\omega)$ of the unperturbed host lattice,

$$P(\omega) = \lim_{\varepsilon \to 0^+} \int_0^\infty du Z(u)/((\omega + i\varepsilon)^2 - u^2)$$
$$= \mathrm{I\!P} \int_0^\infty du Z(u)/(\omega^2 - u^2) - \frac{i\pi}{2\omega} Z(\omega). \tag{3.7}$$

Here $\mathrm{I\!P}$ denotes that the principal part of the integral is taken.
The perturbed Green function G satisfies a Dyson equation. For a single mass defect the perturbation matrix V has one non-vanishing element at the mass-defect site, which is also the neutron scatterer, and the perturbation parameter is

$$\lambda = 1 - m/M \tag{3.8}$$

where m is the defect mass. Dyson's equation

$$G = (1 - PV)^{-1} P$$

is particularly simple given that V has just one element. Moreover, because $P_{\alpha\beta}$ is diagonal in the Cartesian labels $G_{\alpha\beta}$ is also. The Green function $G_{\alpha\beta}(a,a;\omega)$ in (3.2) is found to be

$$G_{\alpha\beta}(a, a; \omega) = \delta_{\alpha\beta} P(\omega)/[1 - \lambda\omega^2 P(\omega)] M \tag{3.9}$$

where $P(\omega)$ is defined in (3.7). It is straightforward to verify that in the limit $\lambda = 0$ we recover from (3.2), (3.3) and (3.9) the standard expression for incoherent scattering from a cubic, harmonic crystal [2].
For $\lambda = 0$ the imaginary part of G is proportional to $Z(\omega)/\omega$. It is therefore a continuous spectrum of states, proportional to $(\omega^2/\omega) = \omega$ in the limit $\omega \to 0$, and finite up to the maximum phonon frequency ω_L. An example $Z(\omega)$ for a realistic model of lattice vibrations, a simple cubic crystal with ratio of sound speeds 0.1, is shown in Fig. 1 together with the Debye spectrum.

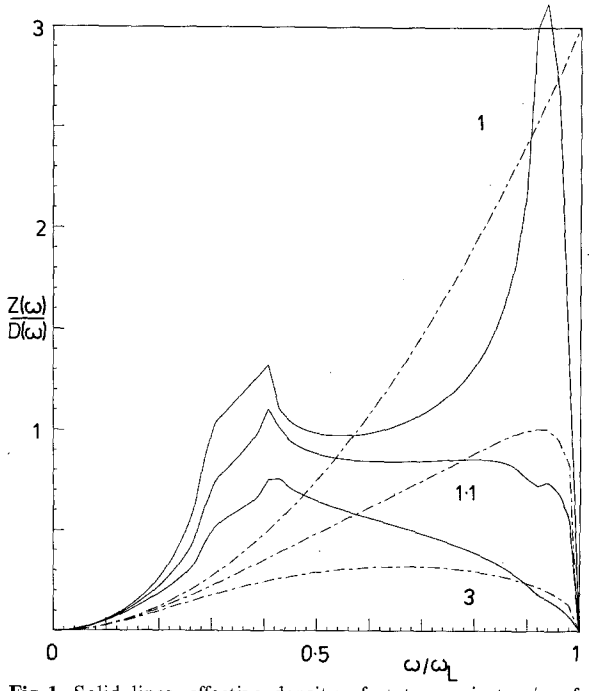

Fig. 1. Solid lines, effective density of states against ω/ω_L for a simple cubic crystal, ratio of sound speeds 0.1. The upper curve is undistorted, the middle has $\omega_0 = 1.1$, $M/m = 1.81$, the lower has $\omega_0/\omega_L = 3$, $M/m = 17.7$. Dashed lines, same for Debye model, except for $\omega_0/\omega_L = 1.1$, $M/m = 1.48$ and $\omega_0/\omega_L = 3$, $M/m = 13.2$

A mass defect $m \neq M$ creates new structure in G that is most significant at frequencies which satisfy

$$1 - \lambda\omega_0^2 \operatorname{Re} P(\omega_0) = 0. \tag{3.10}$$

The frequency ω_0 corresponds to a true bound state of the mixed system if $\omega_0 > \omega_m$, i.e. its frequency lies above the continuum of lattice modes. Thus situation prevails for $m < M$, the case of special interest to us.
In this instance there is a separate contribution from the bound state to the correlation function in $F_a(\mathbf{Q}; t)$, and the latter is the product of factors that arise from an undamped oscillator of frequency ω_0, and a continuum of lattice states of a defect. However, the defect motion necessarily modifies the density of lattice vibrations, and there is a local lattice density of states [2, 7].

$$Z(\omega)/D(\omega) \tag{3.11}$$

where

$$D(\omega) = |1 - \lambda\omega^2 P(\omega)|^2. \tag{3.12}$$

In Fig. 1 we show this local density of states, for the Debye and the realistic models of lattice vibrations, and at bound-state frequencies just above $(1.1\omega_L)$ and well above $(3\omega_L)$ the band of lattice modes. The

lattice density of states is depleted by the formation of the bound state, and this depletion is mainly from the higher frequencies, which is a consequence of the defect perturbation being only in mass, with no change in force constants. The total amount of this depletion is determined by the function $h(\omega_0)$ defined by

$$\frac{Mh(\omega_0)}{2m\omega_0}=P(\omega_0)\left\{\lambda\frac{\mathrm{d}}{\mathrm{d}\omega}\omega^2P(\omega)\Big|_{\omega_0}\right\}^{-1}. \tag{3.13}$$

Because the total number of states is unchanged by substitution of a lattice mass a finite value of $h(\omega_0)$ results in a depletion of states in the perturbed lattice. This is expressed through a normalisation of the local density of states (3.11) obtained from the sum rule (2.4). We find,

$$\int_0^\infty \mathrm{d}\omega Z(\omega)/D(\omega)=\frac{M}{m}(1-h(\omega_0))=H_0(\omega_0). \tag{3.14}$$

For $M=m$, $h(\omega_0)=0$, $D(\omega)=1$ (cf. (3.12)), and (3.14) expresses normalisation of the unperturbed host density of states.

Using (3.9) in (3.2) and taking $m\leqq M$, so a bound state (undamped oscillator) exists, we find the expression (4.4) for the correlation function.

4. Numerical Method

We summarise the steps for calculating the scattering response $S(Q,\omega)$:

$$f(\omega)=\int_0^\infty \mathrm{d}uZ(u)(1-u^2/\omega^2)^{-1}, \tag{4.1}$$

$$h(\omega_0)=\lambda^{-1}(\lambda^{-1}-1)\left\{\int_0^\infty\frac{\mathrm{d}uZ(u)}{(\omega/u-u/\omega)^2}\right\}^{-1}, \tag{4.2}$$

$$D(\omega)=[1-\lambda f(\omega)]^2+[\tfrac{1}{2}\lambda\omega\pi Z(\omega)]^2, \tag{4.3}$$

$$F_a(Q,t)=\exp\left\{\frac{Q^2h(\omega_0)}{2m\omega_0}J(\omega_0,t)+\int_0^\infty\frac{\mathrm{d}uZ(u)J(u,t)}{uD(u)}\right\}, \tag{4.4}$$

$$S(Q,\omega)=\frac{1}{2\pi}\int_{-\infty}^{\infty}\mathrm{d}tF_a(Q,t)\mathrm{e}^{-\mathrm{i}\omega t} \tag{4.5}$$

where $J(\omega,t)$ is defined in (3.13), $Z(\omega)$ is the density of states of a perfect cubic lattice with mass M at each site, m is the defect mass, and $\lambda=1-m/M$.

The frequency ω_0 of the defect mode satisfies

$$\lambda f(\omega_0)=1. \tag{4.6}$$

In Fig. 2 is plotted the relationship between ω_0/ω_L and m/M, for the realistic and the Debye lattice density of states. As $m/M\to 1$, the defect disappears

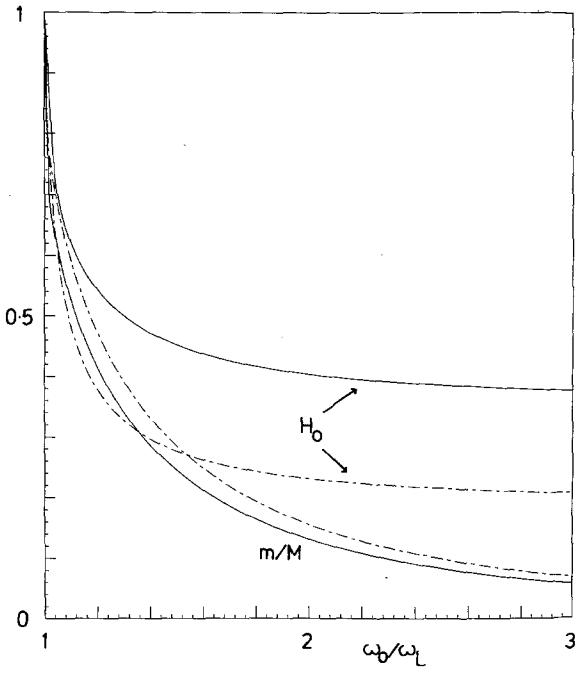

Fig. 2. Lower curves are mass ratio m/M, upper curves the moment $H_0(\omega_0)$ from (3.14), plotted against ω_0/ω_L. Solid lines, simple cubic, dashed lines, Debye model

and $\omega_0/\omega_L\to 1$. For a very light defect, the defect and lattice timescales separate, and we have m proportional to ω_0^{-2}, just as for any harmonically bound mass such as a simple pendulum.

Also plotted in Fig. 2 is the quantity in (3.14), the fraction of modes associated with the lattice after depletion by the bound state. We shall see later that this quantity is related to the width and shift of peaks in the response.

The scattering response is the Fourier transform of the exponential of a Fourier transform, which we evaluate by a sequence of convolutions. We first discretise the frequency, as it must be in any numerical scheme, with spacing h. The density of states can then be approximated as

$$Z(\omega)=\sum_{j=1}^{N}Z_j\delta(\omega-\omega_j);\qquad \omega_j=jh. \tag{4.7}$$

The normalisation can be written $\sum Z_j=1$, so that integrals become sums. For any function $B(\omega)$

$$\int \mathrm{d}\omega Z(\omega)B(\omega)\to\sum_j Z_jB(\omega_j). \tag{4.8}$$

We assume that the defect frequency ω_0 is an exact multiple of h: $\omega_0=hj_0$. This can easily be achieved by making the light mass m dependent on ω_0 rather than solving the transcendental equation (4.6).

We can now write $F_a(Q,t)$ as

$$F_a(Q,t)=\exp\sum_{j=1}^{N+1}A_jJ(\omega_j,t), \tag{4.9}$$

$$A_j=\frac{Q^2}{2M\omega_j}\frac{Z_j}{D(\omega_j)};\quad j=1\text{ to }N$$
$$A_{N+1}=\frac{Q^2}{2M\omega_0}h(\omega_0);\quad \omega_{N+1}\equiv\omega_0. \tag{4.10}$$

It is shown in reference [2] that the scattering amplitude from a single frequency Ω of amplitude A is

$$S(Q,\omega)=\frac{1}{2\pi}\int_{-\infty}^{\infty}\mathrm{d}t\,\mathrm{e}^{-\mathrm{i}\omega t}\mathrm{e}^{AJ(\Omega,t)}$$
$$=\sum_{-\infty}^{\infty}\bar{I}_n(A,\beta\Omega/2)\delta(\omega-n\Omega) \tag{4.11}$$

where the coefficients $\bar{I}_n(A,x)$ are defined in terms of regular modified Bessel functions:

$$\bar{I}_n(A,x)=\mathrm{e}^{-A\coth x+nx}I_n(A/\sinh x). \tag{4.12}$$

The scattering from a sum such as (4.9) can be obtained by successive convolution of the individual terms.

It we let $S^{(k)}(Q,\omega)$ be the scattering corresponding to the correlation function

$$F^{(k)}(Q,\omega)=\exp\sum_{j=1}^{k}A_jJ(\omega_j,t) \tag{4.13}$$

then

$$S^{(k)}(Q,\omega)=\sum_{-\infty}^{\infty}\bar{I}_n(A_k,\beta\omega_k/2)S^{(k-1)}(Q,\omega-n\omega_k). \tag{4.14}$$

Discretising this sequence of scattering amplitudes:

$$S^{(k)}(Q,\omega)=\sum_{j=-\infty}^{\infty}S_j^{(k)}\delta(\omega-jh) \tag{4.15}$$

gives the numerical scheme,

$$S_j^{(k)}=\sum_{-\infty}^{\infty}\bar{I}_n(A_k,\beta\omega_k/2)S_{j-nk}^{(k-1)};\quad S_j^{(0)}=\delta_{j0}. \tag{4.16}$$

The final vector $S_j^{(k+1)}$ is the discretised scattering amplitude from all the different normal mode frequencies of the lattice, including the defect state. It would be as exact as the discretisation of $Z(\omega)$, except for the necessary truncation of the frequency space for the $S_j^{(k)}$. This can be monitored by the sum rule

$$1=\int\mathrm{d}\omega S(Q,\omega)\simeq\sum_j S_j^{(k)} \tag{4.17}$$

which falls short if the truncation is too severe.

The numerical sum rule can be shown by summing (4.16) over j:

$$\sum_j S_j^{(k)}=[\sum_n\bar{I}_n(A_k,\beta\omega_k/2)]\sum_j S_j^{(k-1)}. \tag{4.18}$$

The sum in the bracket is unity by the generating function for modified Bessel functions [6], and $\sum S_j^{(0)}=\sum\delta_{j0}=1$. The numerical version of the f-sum-rule can be shown by differentiating this generating function

$$\sum_j\omega_jS_j^{(N+1)}=\frac{Q^2}{2M}\sum_j\frac{Z_j}{D(\omega_j)}+\frac{Q^2}{2m}h(\omega_0)\simeq\frac{Q^2}{2m}. \tag{4.19}$$

We need the functions $f(\omega)$ and $h(\omega_0)$, which are integrals over the density of states. These should be consistent with the approximation (4.7); for example

$$f(\omega_k)=\sum_j Z_j(1-j^2/k^2)^{-1} \tag{4.20}$$

but this is insufficient when $j=k$. We instead approximate $Z(\omega)$ by linear interpolation between discretisation points, and evaluate f exactly in that sense.

We also need an algorithm for the coefficients $\bar{I}_n(A,x)$, which can be calculated by the recursion relations

$$\bar{I}_{n-1}=\frac{n}{A}(1-\mathrm{e}^{-2x})\bar{I}_n+\mathrm{e}^{-2x}\bar{I}_{n+1}, \tag{4.21a}$$

$$\bar{I}_{n+1}=-\frac{n}{A}(\mathrm{e}^{2x}-1)\bar{I}_n+\mathrm{e}^{2x}\bar{I}_{n-1}. \tag{4.21b}$$

The downward recursion is stable for n positive, the upward for n negative. We start from arbitrary initial conditions at large positive n, and apply (4.21a) to obtain $\alpha\bar{I}_0$, $\alpha\bar{I}_1$, $\alpha\bar{I}_2$, ... for some normalisation α. Similarly using (4.21b) we obtain $\gamma\bar{I}_0$, $\gamma\bar{I}_{-1}$, $\gamma\bar{I}_{-2}$, ... for some γ. Since $\sum\bar{I}_n=1$ and $\alpha/\gamma=\alpha\bar{I}_0/\gamma\bar{I}_0$, we get α and γ, and hence $\bar{I}_n$ from large negative n to large positive n. This set of $\bar{I}_n$ is calculated for each point in the discretisation of the density of states, and also for the defect frequency, and a convolution carried out each time.

A final stage is the convolution of $S_j^{(N+1)}$ with a Lorentzian to give the finite resolution present in experiment. More efficiently we put the resolution function in $S_j^{(0)}$ instead of δ_{j0}, since convolution is commutative.

5. Results

The scattering response is a function of Q and ω, the momentum and energy transfers. It also depends on

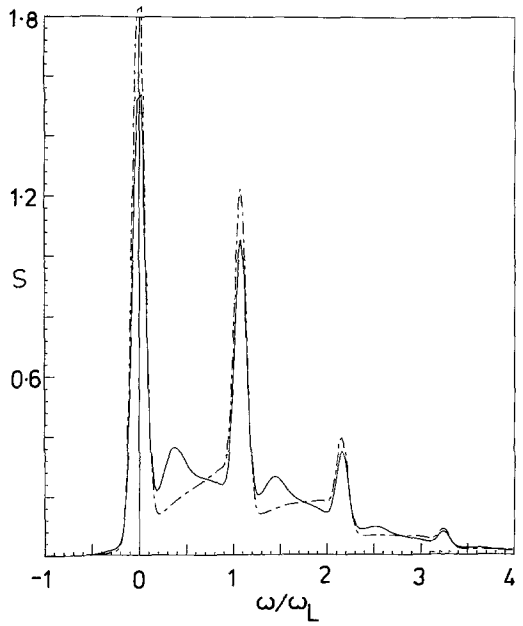

Fig. 3. Scattering response for $\omega_0/\omega_L=1.1$, $T/\omega_L=0.1$, $Q^2/2m\omega_L=1$, for simple cubic (solid) and Debye (dashed). The resolution is $0.2\,\omega_L$

the defect frequency ω_0 or mass ratio m/M, which are related by (4.6), the temperature, and the density of states, of maximum frequency ω_L. The procedure of Sect. 4 gives $S(Q,\omega)$ for constant Q, and we shall summarise its behaviour, which is described in detail in reference [2, 7].

At low momentum transfer, the Sjolander approximation [8, 9] is valid for the scattering from the lattice, and this structure is repeated at multiples of the defect frequency ω_0. Figure 3 shows the response in this regime for $\omega_0=1.1\,\omega_L$: the one-phonon structure $0\leqq\omega/\omega_L\leqq1$ is essentially a copy of the appropriate local density of states of Fig. 1, and the strength of the peaks is given by an expression such as (4.11). The peaks have been broadened from their ideal delta-function shape, by a Lorentzian of width $0.2\,\omega_L$.

As the momentum transfer increases, the delta-function oscillator peaks decrease relative to the smooth lattice background, as multiphonon effects compete with single phonon scattering. The total strength in these oscillator peaks is a lattice Debye-Waller factor [2, 7]:

$$e^{-2W_L}=\exp\left\{-\frac{Q^2}{2M}\int_0^\infty\frac{Z(u)\coth\beta u/2}{uD(u)}\,du\right\}, \tag{5.1}$$

$$=\begin{cases}\exp-\dfrac{Q^2}{2M\omega_L}\displaystyle\int_0^\infty\frac{Z(u)}{D(u)}\frac{\omega_L}{u}\,du; & 2T\ll\omega_L\\[2ex] \exp-\dfrac{TQ^2}{M\omega_L}\displaystyle\int_0^\infty\frac{Z(u)}{D(u)}\frac{\omega_L^2}{u^2}\,du; & 2T\gg\omega_L.\end{cases} \tag{5.2}$$

Table 1. Moments of the effective density of states for the Debye model and for the realistic simple cubic structure, for the limits $M/m\to1$ and $M/m\to\infty$

Moment	Debye $M/m\to\infty$	Cubic $M/m\to\infty$	Debye $M/m=1$	Cubic $M/m=1$
H_{-2}	1.33	2.69	3	4.68
H_{-1}	0.40	0.81	1.5	1.83
H_0	0.19	0.36	1	1
H_1	0.11	0.19	0.75	0.66

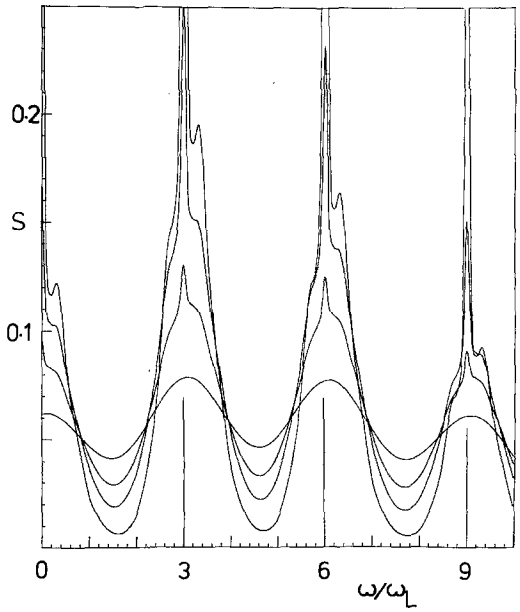

Fig. 4. Scattering response for $\omega_0/\omega_L=3$, $Q^2/2m\omega_L=5$ for simple cubic crystal. The temperature is ω_L (upper curve), $2\omega_L$, $3\omega_L$, $4\omega_L$ (lower smooth curve). The resolution is 0.1 ω_L and the vertical lines are at the unperturbed frequencies, $n\omega_0$, and thus indicate the peak shift

In Table 1 are various moments of the local density of states, defined as

$$H_k(\omega_0)=\int_0^\infty\frac{Z(u)}{D(u)}\left(\frac{u}{\omega_L}\right)^k du. \tag{5.3}$$

These dimensionless functions are given for the Debye model and for the simple cubic structure, in the limits of very light defect, and for $M/m=1$, which is no defect at all. This transition from the Sjolander limit to a set of Gaussians at multiples of the defect frequency is illustrated in Fig. 4, which shows temperatures $T/\omega_L=1,2,3,4$ and the Debye-Waller total peak strength from 0.21 to 0.002. For the upper (low temperature) curve, a small peak from the local density of states (Fig. 1) accompanies each oscillator peak, and for the lower (high temperature) curve, the lattice structure is washed out, leaving a set of

Gaussians. The vertical lines in Fig. 4 are to show that each Gaussian is shifted from a multiple of ω_0, and we shall now investigate this shift, and the width of the Gaussians.

When the defect is very light, its frequency is much greater than the lattice phonons, and we can separate the time scales; the correlation function is a product of a defect correlation function

$$\exp\left\{\frac{Q^2}{2m\omega_0}J(\omega_0,t)\right\} \tag{5.4}$$

and one for the vibrations of the lattice

$$\exp\left\{\frac{Q^2}{2M}\int_0^\infty \frac{du Z(u)}{uD(u)}J(u,t)\right\}. \tag{5.5}$$

This latter correlation function varies slowly and implies a Gaussian response function, which is then repeated at multiples of ω_0 by the former. Expanding the argument of the exponential (5.5) to second order in time gives the response

$$S_L(Q,\omega)\simeq(2\pi\gamma^2)^{-\frac{1}{2}}\exp\left[-(\omega-\omega^*)^2/2\gamma^2\right]$$

and this is combined with (5.4) to give a set of Gaussians

$$S(Q,\omega)=\sum_n \bar{I}_n(y,\beta\omega_0/2)S_L(Q,\omega-n\omega_0)$$
$$y=\frac{Q^2h(\omega_0)}{2m\omega_0}. \tag{5.7}$$

In the expression for S_L, the shift and width are given by [7]

$$\left.\begin{matrix}\gamma^2\\ \omega^*\end{matrix}\right\}=\frac{Q^2}{2M}\int_0^\infty \frac{du Z(u)}{D(u)}\left\{\begin{matrix}u\coth\beta u/2\\ 1.\end{matrix}\right. \tag{5.8}$$

The integral for the shift is that part of the density of states that has not been depleted by the bound (defect) state, and is given by the f-sum rule (3.14). This is plotted for the Debye model and for the simple cubic lattice in Fig. 2, and the light mass limits shown in Table I as H_0. The width is

$$\gamma^2=\begin{cases}\dfrac{Q^2\omega_L}{2M}H_1(\omega_0); & 2T\ll\omega_L\\ \dfrac{TQ^2}{M}H_0(\omega_0); & 2T\gg\omega_L.\end{cases} \tag{5.9}$$

The latter expression gives a FWHM of 2.12 ω_L for the high temperature curve of Fig. 4.

The high Q limit of the response is just a single broad peak, when the scatterer (the defect) is essentially a free particle [9]. The set of oscillator peaks is washed out when the width γ becomes greater than the separation ω_0. This broad peak can then be approximated as a Gaussian with the same derivation as (5.6), but with no separation of timescales;

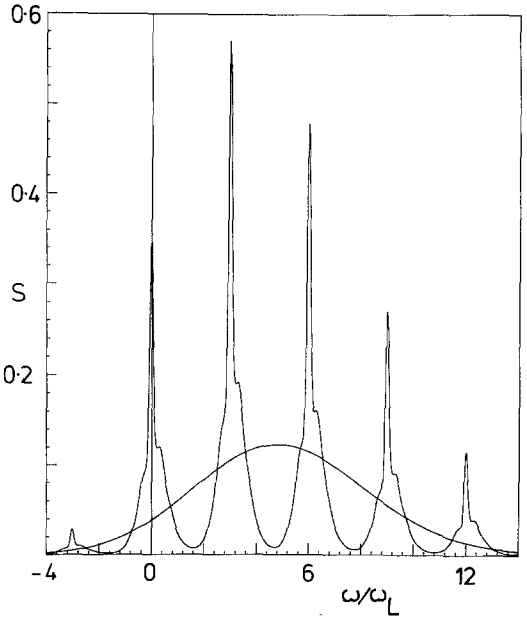

Fig. 5. Scattering response for simple cubic crystal with $Q^2/2m\omega_L=5$ and $T/\omega_L=1$. The peaked curve is $\omega_0/\omega_L=3$, $(M/m=17.7)$, and the smooth curve is $\omega_0/\omega_L=1.1$, $(M/m=1.81)$

$$S(Q,\omega)\simeq(2\pi\Gamma^2)^{-\frac{1}{2}}\exp\left[-(\omega-\Omega^*)^2/2\Gamma^2\right], \tag{5.10}$$

$$\Omega^*=\frac{Q^2}{2M}\left\{h(\omega_0)+\frac{m}{M}\int_0^\infty\frac{du Z(u)}{D(u)}\right\}=\frac{Q^2}{2M}, \tag{5.11}$$

$$\Gamma^2=\frac{Q^2}{2m}h(\omega_0)\coth\beta\omega_0/2+\frac{Q^2}{2M}\int_0^\infty\frac{du Z(u)}{D(u)}u\coth\beta u/2. \tag{5.12}$$

The second equality in (5.11) is the f-sum rule, and states that the average neutron energy loss is the energy of its momentum transfer. The width is for high temperatures

$$\Gamma^2=\frac{TQ^2}{m};\quad 2T\gg\omega_L. \tag{5.13}$$

This is plausible, since in the impulse approximation $\Gamma^2=\langle(\mathbf{V}\cdot\mathbf{V})^2\rangle$, where $\mathbf{V}$ is the scatterer velocity, and by equipartition the energy in each component of $\langle\mathbf{V}\cdot\mathbf{V}\rangle$ is T/m, so $\Gamma^2=Q^2\langle V_q^2\rangle=Q^2T/m$.

Figure 5 illustrates the response from a very light defect $M/m=17.7$ with dominant oscillator peaks, and the local density of states still visible, and the response from a heavier defect $M/m=1.8$. At this momentum transfer, the lighter mass can react much faster, causing the great discrepancy between these curves.

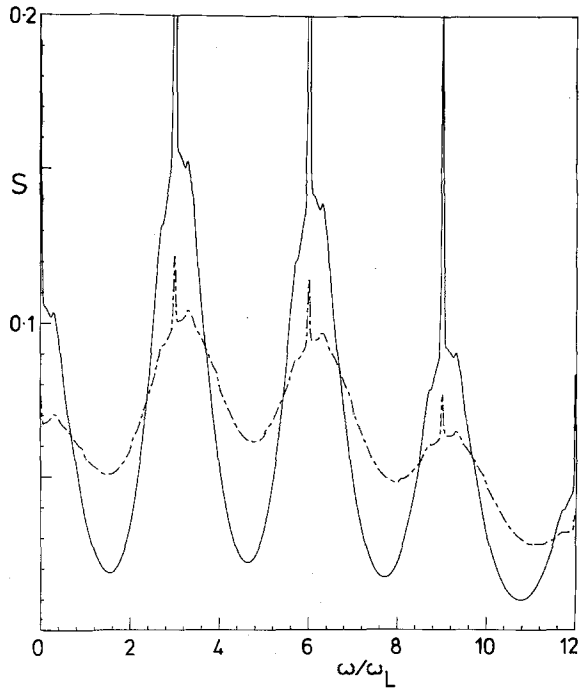

Fig. 6. Exact scattering response (solid line) and uncoupled approximation (dashed line), for the simple cubic crystal, $\omega_0/\omega_L=3$, $T/\omega_L=2$ and $Q^2/2m\omega_L=5$

We now consider an approximation to the response function, which is to replace the phonons of the defected matrix by those of a perfect translationally invariant matrix, and to consider the defect motion uncoupled from the lattice. Formally this consists of setting $Z(\omega)/D(\omega)\to Z(\omega)$ and $h(\omega_0)\to 1$. The local density of states Z/D is not amplitude-weighted; indeed we have chosen cubic crystals precisely to remove the necessity for amplitude-weighting. Neither is it the density of states of the defected crystal; this paper is concerned with the low concentration limit, so the gross density of states is unchanged. The quantity Z/D expresses how the defect velocity is correlated with itself at later times; i.e. how the lattice eigen vectors are distorted near the defect.

This uncoupled approximation makes all the moments $H_k(\omega_0)$ independent of ω_0 and equal to their values at $M/m=1$. The greatest effect of the approximation thus occurs for a very light defect. Since the approximation decouples the phonon spectrum from the defect motion, the narrow oscillator peaks persist longer: Q need only be half as large in the approximation (from (5.2) and Table 1) to wash these out. In addition, the width γ of (5.6) is 3.5 times as great in the uncoupled approximation. These effects are illustrated in Fig. 6, which shows the exact and uncoupled response functions intermediate between the Sjolander regime and a set of Gaussians. It is clear that the uncoupled approximation gives a much larger width, and much smaller peak strength. In the very high Q limit, when the response is a single broad Gaussian, the effects of the approximation are more pronounced. From (5.12), we find the peak to be centred at

$$\Omega^*=\frac{Q^2}{2m}\to\frac{Q^2}{2m}\left(1+\frac{m}{M}\right) \tag{5.14}$$

which violates the f-sum rule result $Q^2/2m$. The high temperature limit of the width becomes

$$\Gamma^2=\frac{TQ^2}{m}\to\frac{TQ^2}{m}\left(1+\frac{m}{M}\right). \tag{5.15}$$

6. Conclusions

We have derived, calculated and described the scattering response from a light defect substituted in a crystal. The numerical method is new, more controllable and more efficient than the conventional Fast Fourier Transform. We have derived the local density of states to be used in the Sjolander approximation, and shown that at higher momentum transfer it is the moments of this Z/D rather than Z that correctly describe the shifts and widths of the Gaussian peaks. The density of states is especially depleted at frequencies near the band edge, because we have chosen to use a mass defect with no change of force constants. We have shown that approximating this local density of states by the lattice density of states is incorrect, especially because of the over-estimation of peak widths.

This model has the advantage of giving the response function in closed form which can be easily calculated, but to be a tool for interpreting neutron scattering data it must be more comprehensive. One could consider different force constants for the defect and for the lattice. A non-zero concentration of defects would broaden the delta-function oscillator peaks of this model. If the defect were interstitial, not substitutional, or if its environment were tetrahedral rather than cubic, there would be several oscillator frequencies, not just one. These complications make the response depend on the generalised density of states, including the phonon eigenvectors, and the algorithm involves matrix operations in place of simple numbers. We feel such an approach would be useful for fitting spectra, perhaps not for understanding.

References

1. Rubin, R.J.: J. Math. Phys. **1**, 309 (1960); ibid. **2**, 373 (1961)
2. Lovesey, S.W.: Theory of neutron scattering from condensed matter. Vol. 1. Oxford: Oxford University Press 1984

3. Maradudin, A.A., Montroll, E.W., Weiss, G.H., Ipatova, I.P.: Theory of lattice dynamics in the harmonic approximation. New York: Academic Press 1971
4. Elliott, R.J., Krumhansl, J.A., Leath, P.L.: Rev. Mod. Phys. **46**, 465 (1974)
5. Taylor, D.W.: Dynamical properties of solids. Maradudin, A.A., Horton, G.K. (eds.), Vol. 2. Amsterdam, Oxford, New York: North-Holland 1975
6. Abramowitz, M., Stegan, I.E.: Handbook of mathematical functions. US Bureau of Standards (1964), Formula (9.6.33)
7. Warner, M., Lovesey, S.W., Smith, J.: Z. Phys. B – Condensed Matter **51**, 109 (1983)
8. Sjölander, A.: Ark. Fys. **14**, 315 (1958)
9. Gunn, J.M.F., Warner, M.: Z. Phys. B – Condensed Matter **56**, 13 (1984)

R.D. Williams
S.W. Lovesey
Rutherford Appleton Laboratory
Science and Engineering Research Council
Chilton, Didcot
Oxfordshire OX11 0QX
United Kingdom